ADVANCES IN ATMOSPHERIC SCIENCES, VOL. 25, NO. 4, 2008, 563–576

A Case Study on the Role of Water Vapor from Southwest China in Downstream Heavy Rainfall

PAN Yang[1,2] (潘 旸), YU Rucong[*1] (宇如聪), LI Jian[1] (李 建), and XU Youping[1] (徐幼平)

[1] *State Key Laboratory of Numerical Modeling for Atmospheric and Geophysical Fluid Dynamics, Institute of Atmospheric Physics, Chinese Academy of Sciences, Beijing* 100029

[2] *Graduate University of Chinese Academy of Sciences, Beijing* 100049

(Received 30 April 2007; revised 14 January 2008)

ABSTRACT

Based on the observation data analysis and numerical simulation, the development of an eastward-moving vortex generated in Southwest China during the period 25–27 June 2003 is studied. The water vapor budget analysis indicates that water vapor in the lower troposphere over Southwest China is transported downstream to the Yangtze and Huaihe River valleys by the southwesterly winds south of the vortex center. A potential vorticity (PV) budget analysis reveals that a positive feedback between latent heat release and low-level positive vorticity plays a vital role in the sudden development and eastward movement of the vortex. Numerical simulations are consistent with these results.

Key words: vortex, potential vorticity, heavy rainfall, water vapor, numerical simulation

DOI: 10.1007/s00376-008-0563-x

1. Introduction

In summer, when southwesterly winds prevail around the Yangtze River valley, synoptic cyclonic disturbances continually appear in the eastern foothills of the Tibetan Plateau and the upper reaches of the Yangtze River. One such circulation system is the southwest (SW) vortex. When it migrates eastward, it can enhance the disturbances on the Meiyu front and cause recurrent heavy rainfall downstream (Tao and Ding, 1981). Hu and Pan (1996) and Gao and Xu (2001) have studied the cyclonic disturbances over the Yangtze River valley arising from the eastward-migrating SW-vortex. Zhang et al. (2003) showed that the 20–30 day low-frequency oscillation of the circulation around the mid-latitudes of East Asia favored the low-pressure systems over the Tibetan Plateau moving eastward to 115°–125°E and strengthening the disturbances on the Meiyu front over the Yangtze River and Huaihe River. Chen et al. (2003) also indicated that the formation, development and eastward-movement of the low-pressure system over the eastern Tibetan Plateau were favorable for the frequent genesis, development and eastward-movement of the SW vortex. It is commonly suggested that the upstream, eastward-moving low-pressure system has significant impacts on the downstream development of the cyclonic disturbances and the associated rainfall over the Yangtze River valley. However, the physical mechanisms involved remain unclear.

Previous studies (Tao and Chen, 1987; Huang et al., 1998; Zhou et al., 2005; Zhou and Yu, 2005) suggest that there are three paths for the water vapor transport contributing to Chinese summer rainfall: one is from the Arab Sea and Bay of Bengal to eastern China by the Indian monsoon; another is from the West Pacific Ocean via the Southeast Asian monsoon; the third is the cross-equatorial flow around 105°–150°E. Which of these plays the most important role in the eastward-moving vortex investigated here remains unclear. It should be noted that, while there has been emphasis on the large-scale moisture transport, less attention has been directed towards the local water vapor in the lower troposphere in Southwest China. Around the eastern foothills of the Tibetan Plateau, the southern Sichuan Basin and the Yunnan-Guizhou Plateau, there is a perpetual center of high relative humidity (>80%) at low levels during the

*Corresponding author: YU Rucong, yrc@cma.gov.cn

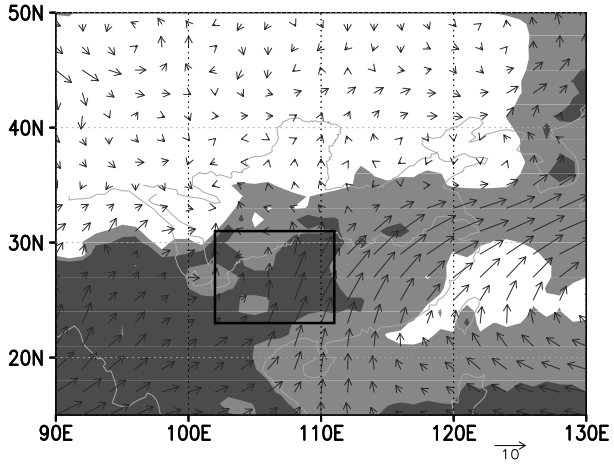

Fig. 1. The 850-hPa relative humidity (light grey: value >70%; heavy grey: value >80%) and vector wind (vector arrow) during the Meiyu period of 2003 (averaged from 21 June to 22 July). The rectangle marks the region—SW in the sensitivity experiments.

Meiyu period of 2003 when the eastward-moving vortices arose frequently (Fig. 1). On the synoptic scale, the water vapor in this area has the most significant impacts on the development of an eastward-moving vortex.

In the summer of 2003, the Huaihe River valley frequently suffered excessively heavy rains which resulted in major disasters. The frequent occurrence of heavy precipitation over the Yangtze River and Huaihe River valleys during the Meiyu period depends heavily on the sustained moisture supply transported from the south by the prevailing southwesterly winds. Assessment of the synoptic evolution during the Meiyu period of 2003 indicates that given the abundant supply of moisture, the eastward-moving vortices play an important role in the generation of heavy rain in the lower reaches of the Yangtze River and Huaihe River. Zhang et al. (2004) and Sun et al. (2004) studied the large-scale atmospheric circulation features during this period, but the synoptic-scale vortices are not considered explicitly.

In order to enhance our understanding of the physical processes underlying the eastward movement, development, and effects on downstream rainfall, the vortex case of late June 2003 was selected for study. Also investigated are the dynamic feedback of the water vapor in Southwest China on the eastward moving vortex and the role of the moisture transport from Southwest China to the areas downstream of the vortex.

Section 2 provides a description and synoptic analysis of the case study. Numerical simulation and sensitivity experiments are discussed in section 3. Conclusions and some further remarks are found in section 4.

2. Case description and synoptic analyses

At 0000 UTC 25 June 2003, a vortex appeared in the northern Sichuan Basin and remained nearly stationary for about one day. Thereafter, it moved eastward and gradually intensified while bringing heavy rains to the Yangtze River and Huaihe River valleys. The two questions addressed in this study are: Why does the upstream vortex develop and migrate eastward, and how does the water vapor in Southwest China affect the rainfall downstream? To answer these questions, synoptic analyses, as well as potential vorticity (PV) diagnosis and water vapor budget analysis are utilized. The synoptic analyses are based upon station sounding data at 12-hour intervals and hourly precipitation amounts automatically recorded by siphon or tipping-bucket rain gauges. The PV diagnostics and water vapor budget analysis are derived from the NCEP (National Centers for Environmental Prediction) gridded $1^\circ \times 1^\circ$ data at 6-hour intervals.

The area around Southwest China east of the Tibetan Plateau, which includes the Sichuan Basin, the upper reaches of the Yangtze River and the Yunnan-Guizhou Plateau, are referred to here as the upstream or the southwest area. The area around the middle-lower reaches of the Yangtze River and the Huaihe River valleys are defined as the downstream area.

2.1 *Synoptic overview and analysis*

The case study here covers a 48-hour period from 0000 UTC 25 June to 0000 UTC 27 June 2003. Figure 2 shows the 850-hPa geopotential height and pseudo-equivalent potential temperature fields during this period. Figure 3 displays the geopotential height and temperature fields at 500 hPa and the positive relative vorticity fields at 850 hPa. At 0000 UTC 25 June, a low pressure was observed in the northern Sichuan Basin (Fig. 2a), associated with a weak cyclonic convergent vortex center (Fig. 3a, triangle). A high moisture center with high pseudo-equivalent potential temperature was located to its south (Fig. 2a, dashed line), enhancing the atmospheric instability over the southwest area. The cyclonic circulation east of the low pressure stretched eastward and merged with the shear line over the lower reaches of the Yangtze River, creating a belt of positive relative vorticity (Fig. 3a, shadow). Twelve hours later (not shown), in response to an upstream low-pressure disturbance along the eastern flank of the Tibetan Plateau, the low pressure slowly strengthened and migrated southeastward to the east of the river basin. At the same time, the southwest moisture center expanded and spun off a

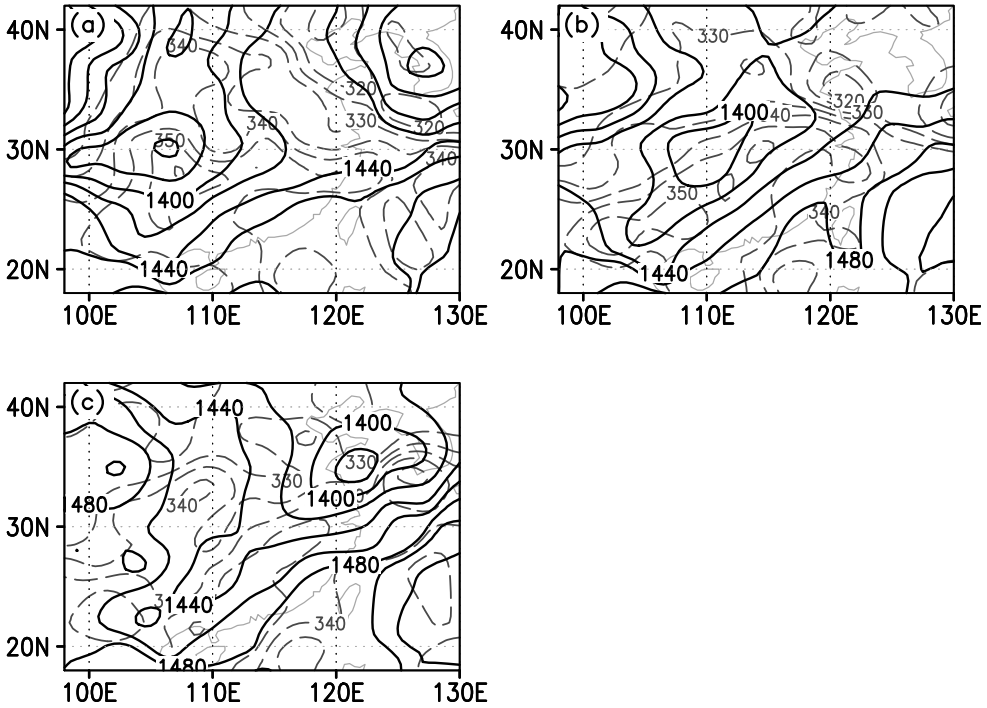

Fig. 2. The synoptic evolution (station observation data): the 850-hPa geopotential height (solid line, units: gpm, interval: 20 gpm) and pseudo-equivalent potential temperature (dashed line, units: K, interval: 5 K) at (a) 0000 UTC 25, (b) 0000 UTC 26, (c) 0000 UTC 27 June 2003.

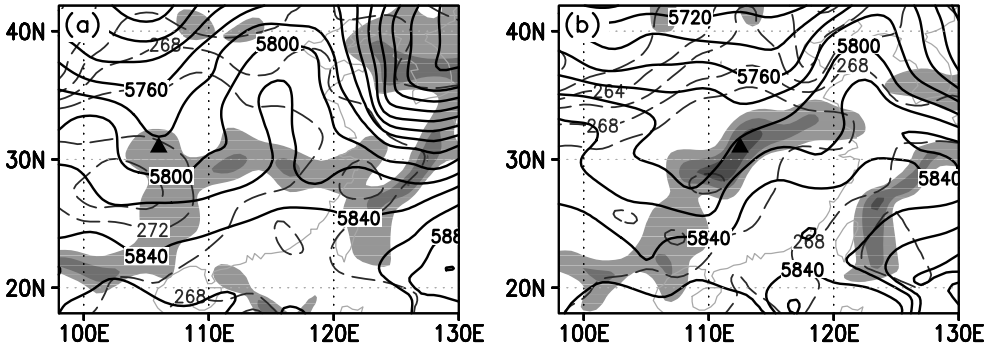

Fig. 3. The geopotential height (solid line, units: gpm), temperature (dashed line, units: K) at 500 hPa and the 850-hPa positive relative vorticity (shadow, value $>1\times10^{-5}$ s^{-1}, interval: 2×10^{-5} s^{-1}) at (a) 0000 UTC 25 and (b) 0000 UTC 26 June 2003. The black triangles mark the vortex centers at 850 hPa at corresponding time.

smaller center to the east, which resulted in a trans-meridional moisture front over the downstream area.

In mid-troposphere, from 0000 UTC 25 to 0000 UTC 26 June, a 500-hPa trough developed and remained stationary east of the Tibetan Plateau (Fig. 3 a and b, solid line). The warm advection east of the trough, just east of the vortex center, was enhanced, and the vortex gradually stretched eastward. By 0000 UTC 26 June the vortex had begun intensifying rapidly (Fig. 3b, shadow), and migrated eastward out of the southwest area (Fig. 2b, solid line; Fig. 3b, triangle). The high moisture center that broke away from the southwest moisture center also moved northeastward with the vortex (Fig. 2b, dashed line).

At 1200 UTC 26 June (not shown), a developing short-wave trough near 36°N, 115°E migrated southward. The cold advection west of the trough increased the baroclinic instability over the Yangtze River and Huaihe River valleys. This contributed further to the eastward-movement of the vortex. Meanwhile, the

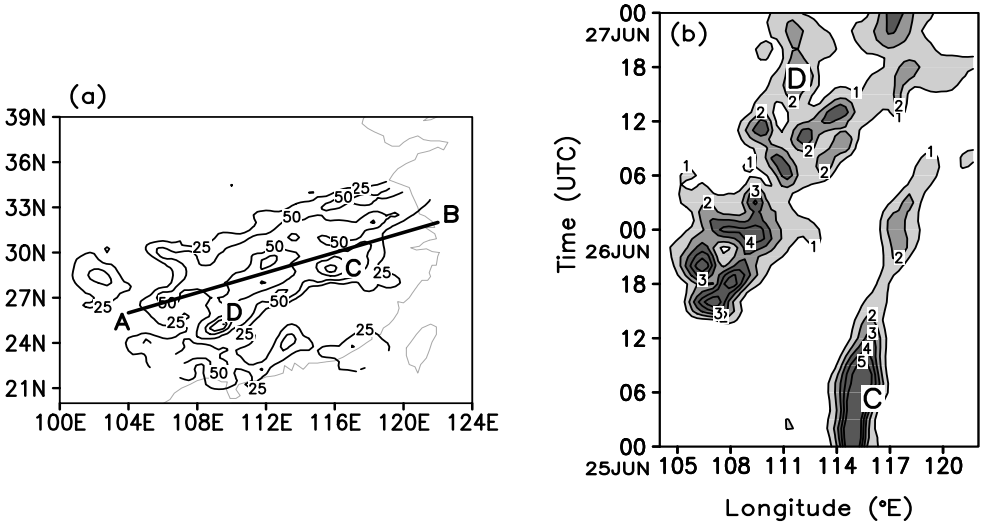

Fig. 4. (a) The observed 48-hour accumulated rainfall (units: mm) from 0000 UTC 25 to 0000 UTC 27 June 2003; (b) the precipitation longitude-time section along line AB on Fig. 4a (units: mm h^{-1}). The sign C and D are the precipitation centers.

trough east of the Tibetan Plateau developed, and the sinking northwesterly cold and dry airflow to the rear of the trough strengthened the cold front to the southwest of vortex center (not shown). At 0000 UTC 27 June, the vortex moved eastward into the Yellow Sea from south of Shandong province on the east coast of China (Fig. 2c).

The synoptic analyses suggest that the stationary 500-hPa trough east of the Tibetan Plateau facilitates the mid-level upward motion over the vortex and cyclonic convergence at low levels which provide favorable dynamics for the vortex. Additionally, the resident low-level moist air in the southwest area provides abundant moist energy for rapid development of the vortex as it migrates into this area. Before the vortex moves out of the southwest area, a high moisture center breaks away from the southwest center towards the east and thereby maintains the developmental potential of the eastward propagating vortex.

Figure 4a presents the observed 48-hour accumulated rainfall from 0000 UTC 25 to 0000 UTC 27 June 2003. The rain-belt was generally oriented southwest-northeast from Southwest China along the middle reaches of the Yangtze River to the Yangtze River and Huaihe River valleys. Most areas along this belt suffered heavy rainfall. The eastern precipitation center, designated C, and the southern center, designated D, exceeded 100 mm. A time-longitude cross section of precipitation along the line AB in Fig. 4a is displayed in Fig. 4b. The precipitation shown here is the meridional average over about 3 degrees of latitude. The precipitation at C actually began before the study period at 1800 UTC 24 June and resulted from the preexisting low-level shear line over the middle and lower reaches of the Yangtze River. The rainfall at this center peaked between 0100–0900 UTC 25 June and, therefore, appears unlikely to have contributed to the eastward-moving vortex. At D the precipitation began about 1400 UTC 26 June and ended at approximately 1900 UTC 26 June. This center resulted primarily from a sequence of relatively brief periods of convective precipitation that developed on the cold front southwest of vortex center as it migrated to the Yangtze River and Huaihe River valleys.

Precipitation related to the vortex extended northeastward from the upper reaches of the Yangtze River to the Yangtze and Huaihe River valleys. From Fig. 4b it can be seen that the precipitation in the southwest area (about 105°–108°E) started about 1400 UTC 25 June and then rapidly increased in intensity reaching sustained peak values between 1600 UTC to 2100 UTC 25. During this period the vortex grew rapidly in Southwest China. After 0000 UTC 26 June, as the mature vortex moved eastward out of the southwest area, the rainfall also stretched eastward to the middle reaches of the Yangtze River. About one day later, the precipitation had migrated to the lower reaches of the Yangtze River and Huaihe River. Evolution of the precipitation pattern in this case is typical of eastward moving vortices.

From the synoptic analysis and precipitation data one can see that the development stage of the vortex is nearly consistent with the evolution of the precipitation pattern as the vortex moves into the southwest area. This suggests that there may be a positive feedback between the latent heat release and the

rapid growth of the vortex over a period of just a few hours. Moreover, development of the precipitation pattern around the vortex center and to its southwest and east as it migrates eastward indicates that the effects of latent heating play an important role in vortex maintenance and movement.

2.2 *Potential vorticity budget analysis*

In order to study the physical mechanisms of vortex development and to further investigate the consistent relationship between the vortex system and precipitation, a potential vorticity (PV) budget analysis was conducted. Assuming diabatic heating is from latent heat release, the PV and PV tendency can be written as:

$$q = -(f+\zeta_p)\frac{\partial\theta}{\partial p} + g\left(\frac{\partial v}{\partial p}\frac{\partial\theta}{\partial x} - \frac{\partial u}{\partial p}\frac{\partial\theta}{\partial y}\right), \quad (1)$$

$$\frac{\partial q}{\partial t} = -\nabla\cdot(q\boldsymbol{V}_{\rm h}) - \frac{\partial}{\partial p}(q\omega) + g\boldsymbol{\zeta}_{\rm a}\cdot\nabla_3\dot{\theta}\,. \quad (2)$$

Here, q represents PV. θ is the potential temperature. $\boldsymbol{\zeta}_{\rm a} = (f\boldsymbol{k} + \nabla_3\times\boldsymbol{V})$ is the three-dimension absolute vorticity, and ζ_p is its vertical component. $\dot{\theta}$ represents the latent heating rate calculated by the method used by Emanuel et al. (1987) and Raymond (1992). The Eq. (2) indicates that contributions to the local PV change arise from horizontal and vertical PV flux divergence and PV redistribution due to latent heating. The latent heating term can be divided into two parts:

$$\boldsymbol{\zeta}_{\rm a}\cdot\nabla\dot{\theta} = \zeta_x\frac{\partial\dot{\theta}}{\partial x} + \zeta_y\frac{\partial\dot{\theta}}{\partial y} - (f+\zeta_p)\frac{\partial\dot{\theta}}{\partial p}\,. \quad (3)$$

One is related to the horizontal gradient in the distribution of the latent heating, referred to as the horizontal effect of latent heating; the second effect arises from the vertical variance of latent heat release. In this case, around the vortex center, the horizontal latent heating effect is almost negative and is about 5 times smaller in magnitude than the vertical latent effect (not shown). Thus, the latent heat forcing of the PV tendency arises mostly from the vertical distribution term.

Figure 5 shows the PV and PV tendency caused by latent heating and horizontal flux convergence averaged between 850 hPa and 750 hPa. During the early stages of vortex development, a high PV center is located over the northern Sichuan Basin in the lower troposphere (Fig. 5a, dashed line). To the southwest of the vortex, northeasterly winds prevail over the basin (not shown). The PV center is superposed by a center of intense latent heating (Fig. 5a, solid line) associated with the aforementioned stationary 500-hPa trough east of the Tibetan Plateau. The ascent, which is generally east of the trough axis, coincides with near-saturated air (relative humidity up to 90%). The resulting condensation of water vapor and latent heat release at mid-tropospheric levels force an increase in PV and intensification of the cyclonic circulation at low levels. This strengthens the northeasterly winds over the basin. Then, almost immediately, orographic lifting of moist air in the western basin triggers convection. However, this center of the latent heat effect is partially offset by the vertical and horizontal PV flux divergence (not shown). To the southwest of the PV center there is strong horizontal PV flux convergence (Fig. 5b, solid line) and, hence, a positive PV tendency (Fig. 5b, dashed line). As a result, six hours later the PV center has moved somewhat to the southwest (Fig. 5c, dashed line).

The 500-hPa trough remains over the eastern Sichuan Basin until 1800 UTC 25 June, with the latent heating effect continuing to intensify the low-level cyclonic circulation. As a result the northeast wind over the basin constantly strengthens and the intensity of convection continues to increase. With intensification of the cyclonic circulation, the increasing northeasterly winds over the basin are turned counterclockwise, which shifts the maximum terrain forcing southeastward along the southern mountains of the basin (not shown). The convection gradually migrates southeast of the basin where it deposits copious amounts of water vapor at low layers. The convection enhances the low-level convergence and upward motion and, thus, the latent heating effect becomes prominent. At 1800 UTC 25 June, an intense latent heating center appears in the southwest area (Fig. 5c, solid line), and the PV correspondingly increases (Fig. 5d, dashed line). With an abundant supply of moisture at low levels, the latent heating effect can produce a positive feedback with vortex development. Hence, the vortex rapidly intensifies which, in turn, further increases the convection. In the section 3.3, the nature of this positive feedback will be further illuminated by the numerical simulation.

After 1800 UTC 25 June, the enhanced low-level cyclonic circulation intensifies the southwesterly winds south of the vortex, which enhances the eastward moisture transport. Consequently, the high moisture center at the southwest area extends to the east of vortex, where convergence and ascent around the vortex center is strongest (not shown). Thus, the maximum latent heating effect also shifts to the east of the vortex (Fig. 5e, solid line), where the vorticity is rapidly increasing (Fig. 5f, dashed line). When the vortex reaches its mature stage, the horizontal PV flux convergence center also shifts to the east of the PV center (Fig. 5f,

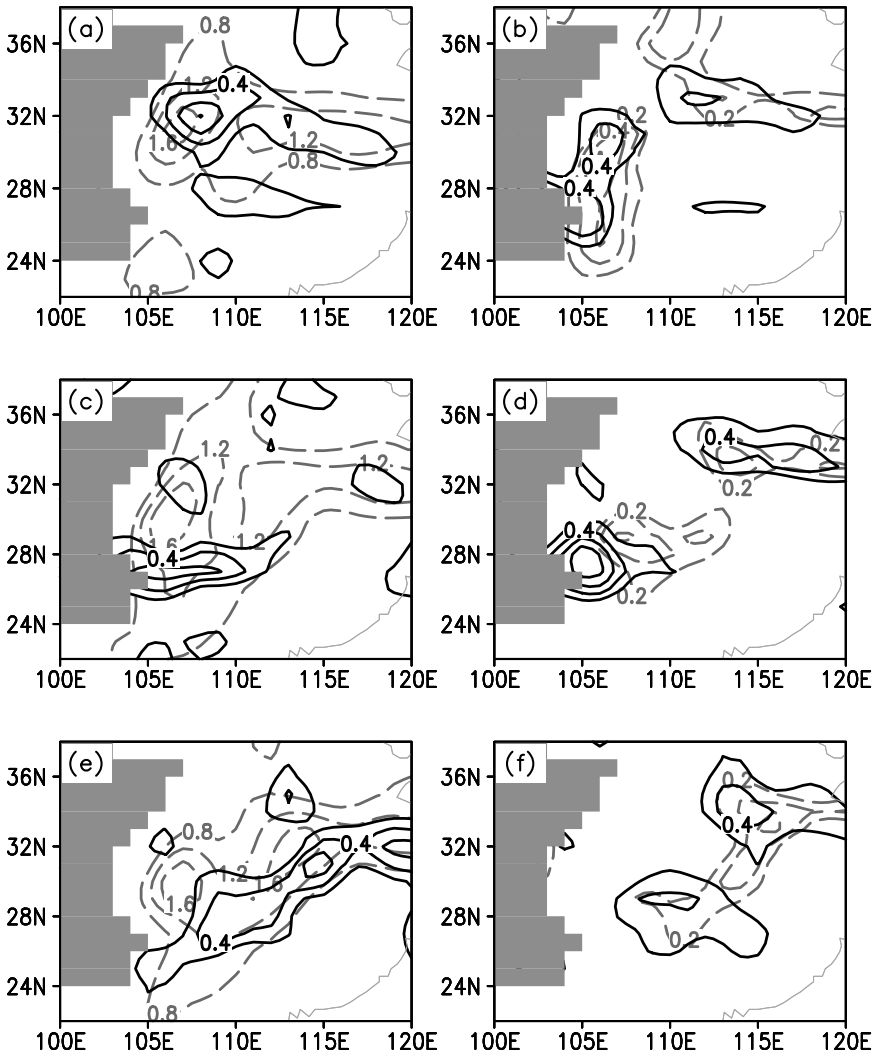

Fig. 5. (a) the PV (dashed line, value >0.8, interval: 0.4, units: PVU, 1 PVU=10^{-6} m^2 s^{-1} K kg^{-1}) and PV change caused by latent heating effect [solid line, value >0.2, interval: 0.2, units: PVU (6 h)$^{-1}$] averaged between 850 hPa and 750 hPa at 1200 UTC 25 June 2003; (b) the PV tendency [dashed line, value >0.2, interval: 0.1, units: PVU (6 h)$^{-1}$] and horizontal PV flux divergence [solid line, value >0.2, interval: 0.2, units: PVU (6 h)$^{-1}$] averaged between 850 hPa and 750 hPa at 1200 UTC 25 June 2003. (c) and (d) are the same as (a) and (b) but at 1800 UTC 25 June 2003. (e) and (f) are the same as (a) and the (b) but at 0000 UTC 26 June 2003. Shadow indicates the area where surface pressure is lower than 850 hPa (represents the terrain).

solid line), and horizontal PV divergence is over and to the northwest of the PV center (not shown). By 0000 UTC 26 June, the vortex has moved eastward out of Southwest China.

From the discussion above, one can see that the combination of the stationary 500-hPa trough and the water vapor source at low levels in Southwest China spur development of the vortex system through latent heating. The eastward migration (Fig. 2) of the high moisture center east of the vortex center and the corresponding prominent center of latent heat release contributes to the eastward motion of vortex. Accompanying development of the cyclonic circulation around the maturing vortex, the horizontal PV flux convergence becomes centered east of the vortex and, therefore, also contributes the eastward propagation of vortex.

2.3 *Water vapor budget analysis*

Aside from the latent heating feedback mechanism in vortex development, a component of the water vapor supply in the southwest area is the downstream

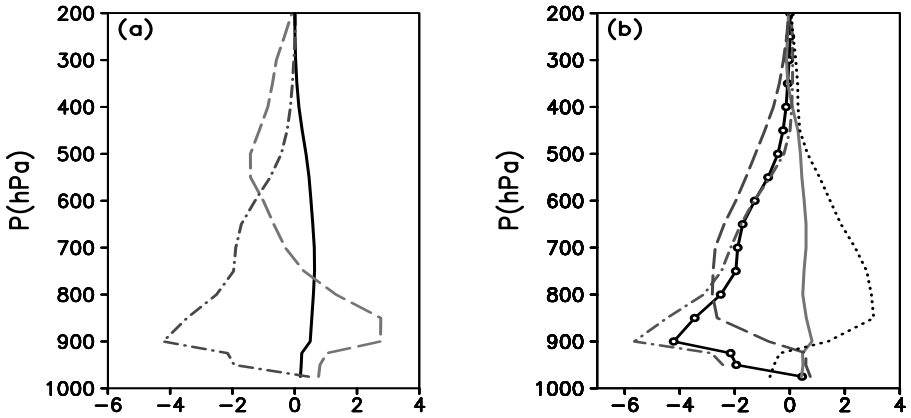

Fig. 6. (a) The vertical distribution of the water vapor budget (solid line: the local water vapor change; dash-dotted line: horizontal water vapor flux divergence; dashed line: vertical water vapor transport; units: 10^7 kg s^{-1}); (b) the vertical distribution of the water vapor fluxes at four boundaries (hollow dot line: horizontal water vapor flux divergence; dash-dotted line: the south boundary, dashed line: the west boundary; solid line: the north boundary; dotted line: the east boundary; units: 10^7 kg s^{-1}) for the region about 28°–35°N, 114°–121°E averaged from 0000 UTC 25 to 0000 UTC 26 June 2003.

transport by the southwesterly winds south of vortex center. To further investigate this transport, a water vapor budget was calculated. The regional averaged water vapor budget equation can be written as:

$$\frac{1}{\sigma g}\int_{p_u}^{p_s}\int_{\sigma}\left(\frac{\partial q}{\partial t}+\nabla\cdot q\boldsymbol{V}_h+\frac{\partial \omega q}{\partial p}\right)dpd\sigma = -m+E_s\,. \tag{4}$$

Here, σ represents the selected region. p_s and p_u are the surface and top atmospheric pressure levels, respectively (1000 hPa and 300 hPa here). $\partial q/\partial t$ is the local water vapor change, $\nabla\cdot q\boldsymbol{V}_h$ is the horizontal water vapor flux divergence, and $\partial\omega q/\partial p$ is the vertical divergence. m and E_s are rates of condensation and evaporation at surface, respectively. The horizontal water vapor flux divergence is generally partitioned into the water vapor fluxes along four lateral boundaries (east, south, west, and north) of the selected region (Ding, 1989).

The region selected for the budget analysis is about 28°–35°N, 114°–121°E, which generally includes the area over the Yangtze River and Huaihe River valleys. Figure 6 presents the vertical distribution of the water vapor budget prior to the vortex exiting the southwest area. The influence of terrain is included in the budget calculation. There is an apparent increase in water vapor from the bottom to 400 hPa resulting from the effects of significant horizontal convergence in the lower troposphere and vertical convergence above 700 hPa (Fig. 6a). From examination of the water vapor fluxes at the lateral boundaries (Fig. 6b), one can see that the most significant contributions are from the south and west boundaries with maxima at 900 hPa and 850–700 hPa respectively. This indicates that the southwesterly winds south of vortex are mainly responsible for the moisture transport into the selected region at low levels. After the vortex moves eastward, the strengthening southwesterly winds distinctly augment the moisture transport through the south and west boundaries. However, the condensation associated with increasing rainfall downstream more than offsets the influx of moisture, such that there is net water vapor decrease (not shown). The analysis above suggests that the condensation and rainfall upstream can subsequently influence the local water vapor content downstream otherwise associated only with the moisture transports through the boundaries.

3. The numerical simulation by AREM

To further enhance our understanding of the positive feedback between the latent heating and the vortex development, and to confirm the importance of the moisture transport from the southwest to the downstream heavy rainfall, numerical simulations by the Advanced Regional Eta-coordinate Model (AREM) are discussed in this section.

3.1 *Introduction of AREM and numerical simulation design*

AREM is a mesoscale forecasting model based on the dynamic frame designed by Zeng (1963). The eta(η)-coordinate is adopted as the vertical coordinate

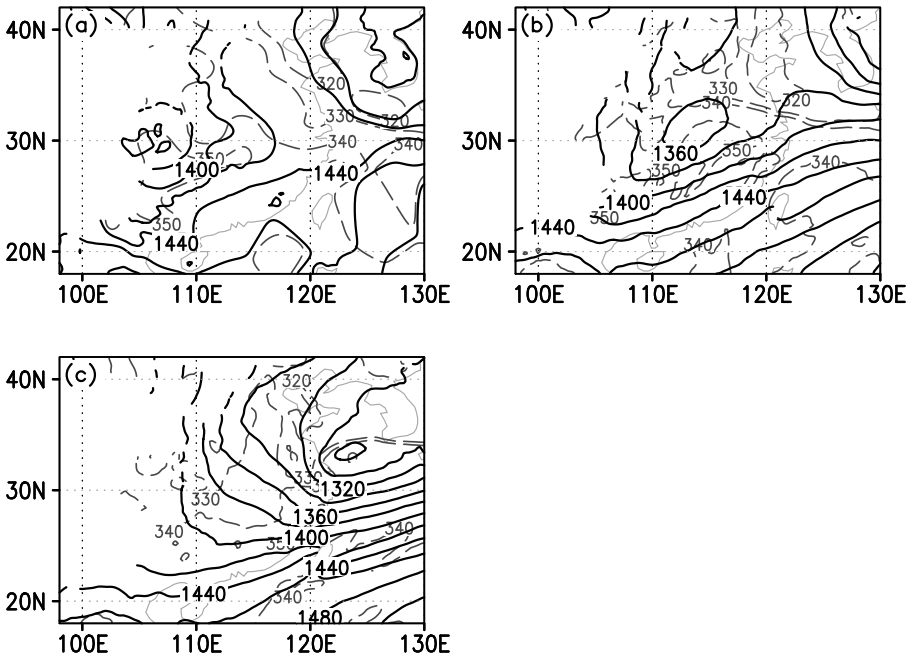

Fig. 7. The same as Fig. 2 but for the simulated results of the control experiment EXP0.

Table 1. The sensitivity experiments schemes.

	Schemes	Purposes
EXP1	Shut off the latent heat release in the whole model region.	Verify the latent heating effect.
EXP2	Keep the relative humidity between 850 hPa and 700 hPa under 70% in the region—SW.	Verify the effect of the water vapor at low levels in the southwest area.
EXP3	Just shut off the latent heat release in the region—SW.	Verify the dynamic feedback of latent heat release in the southwest area.

(Mesinger, 1984). A two-step shape-preserving advection finite difference scheme is designed to keep a reasonable moisture advection (Yu, 1994, 1995). In recent years, the model has done well in the prediction of the heavy rainfalls over the Yangtze River and Huaihe River valleys (Yu and Xu, 2004). In the control run (called EXP0), the model domain covers 15°–50°N, 90°–130°E, with a 15-km horizontal resolution and 32 uneven vertical levels from the surface to 10 hPa. The physical processes include the explicit prognostic warm cloud scheme (Xu et al., 1998), modified Bett's (1986) convective adjustment scheme, a nonlocal diffusion planetary boundary layer parameterization scheme (Holtslag and Boville, 1993), a multistratification profile-flux scheme (Zeng et al., 1998), and a radiation scheme (Ghan et al., 1982). The initial fields are derived from Barne's (1973) objective analysis of station sounding data. The model is integrated from 0000 UTC 25 June 2003 (defined as $\tau 00$) to 0000 UTC 27 June 2003 ($\tau 48$), and hourly simulation data are used for analysis.

Three numerical sensitivity experiments were designed, as listed on Table 1. In EXP1, latent heat release is neglected over the entire model domain to assess the effect of the latent heating feedback mechanism. In EXP2, the relative humidity is limited to a maximum value of 70% between 850 hPa and 700 hPa over the region-SW (23°–31°N, 102°–111°E) marked in Fig. 1. This experiment is designed to examine the importance of the water vapor transport into the downstream region from the southwest. EXP3 is same as EXP1, except it is only run for the region-SW in order to examine the feedback effects in that region alone.

3.2 *Analysis on the results in EXP0*

Figure 7 is the same as Fig. 2, except for the numerical results in EXP0. In comparison with observations, the simulation reproduces the evolution of the vortex well as it first develops in Southwest China, and subsequently moves downstream (Fig. 7, solid line). The model also correctly predicts the characteristics of

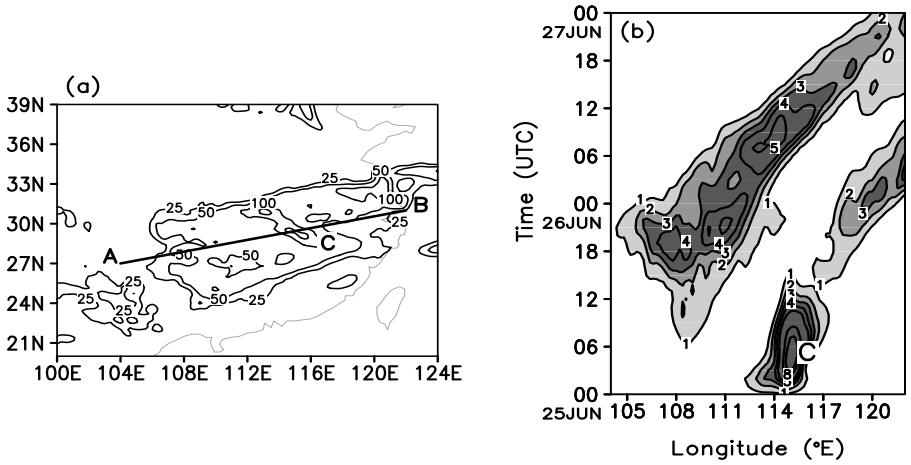

Fig. 8. (a) The 48-hour accumulated rainfall simulated by EXP0 (units: mm) from 0000 UTC 25 (τ00) to 0000 UTC 27 (τ48) June 2003; (b) the precipitation longitude-time section along line AB on Fig. 8a (units: mm h^{-1}). The sign C is the precipitation center.

the eastward movement of warm moist air in the southwest area associated with the vortex and the moisture frontogenesis ahead of the vortex (Fig. 7, dashed line). The cyclonic circulation along the cold front to the southwest of vortex, however, is somewhat weaker in the last 12-hours of the simulation.

Figure 8a shows the 48-hour accumulated rainfall from 0000 UTC 25 June to 0000 UTC 27 June in EXP0. The northeast-southwest oriented pattern and position of the rain-belt are very similar with those observed (Fig. 4a). But at location C, the model produces notably smaller amounts of rain and places it somewhat south of the observed center. In the observations, the rain at this center starts at night on 24 June and reaches its maximum intensity near the beginning of the simulation. Due to model spin-up problems, the simulated intensity of the precipitation, not unexpectedly, is somewhat weaker than observed at the start of the integration. Also, because of a weaker cold front in EXP0, the observed convective precipitation center (D in Fig. 4a) is not predicted very well. However, the model does simulate the much heavier rainfall around the vortex center as it moves to the lower reaches of the Yangtze River and Huaihe River.

The longitude-time cross section of precipitation along line AB in Fig 8a (Fig. 8b) shows that the simulation generates a pattern very similar with the observations (Fig. 4b). The model catches the rainfall associated with the eastward-moving vortex and simulates the precipitation in the southwest area which develops at around 1500 UTC 25 June and peaks about 2100 UTC 25 June. When the vortex moves out of the southwest area, the associated precipitation in the model migrates eastward and redevelops from 0600 UTC 26 June around 111°–114°E. This evolution is very similar to that observed, although the simulated rainfall is heavier and its eastward-movement is somewhat faster.

Overall, the AREM provides a reasonable simulation. The model well reproduces the eastward movement of the vortex and the associated rainfall, although with some errors in depicting the vortex system and associated precipitation patterns. It also simulates reasonably the PV disturbance at 500 hPa associated with the 500 hPa trough (not shown).

3.3 *Physical understanding on the development and movement of vortex*

The preceding analyses suggest there is a positive feedback between the latent heat release and intensification of the vortex. To investigate further a PV budget analysis was performed on the high spatial-and-temporal resolution output from the model simulation in order to diagnose the influence of latent heat release on the PV tendencies. The latent heating term of Eq. (2) is determined directly from the latent heating rate from the model and partitioned into its horizontal and vertical components.

Figure 9 shows the time-height sections of PV and the PV budget terms averaged over an area of $1° \times 1°$ centered on the position of the 850-hPa vorticity maximum (31.2°N, 114°E) at τ27. The low-level PV slowly increases beginning at τ15 and is confined initially to below 800 hPa (Fig. 9a). Just over 6 hours later, the PV begins to increase very rapidly from the surface to 600 hPa reaching peak values at τ26 (Fig. 9b). Qualitatively, the total diagnosed PV tendency (Fig. 9b) follows this evolution quite closely. By comparing Figs.

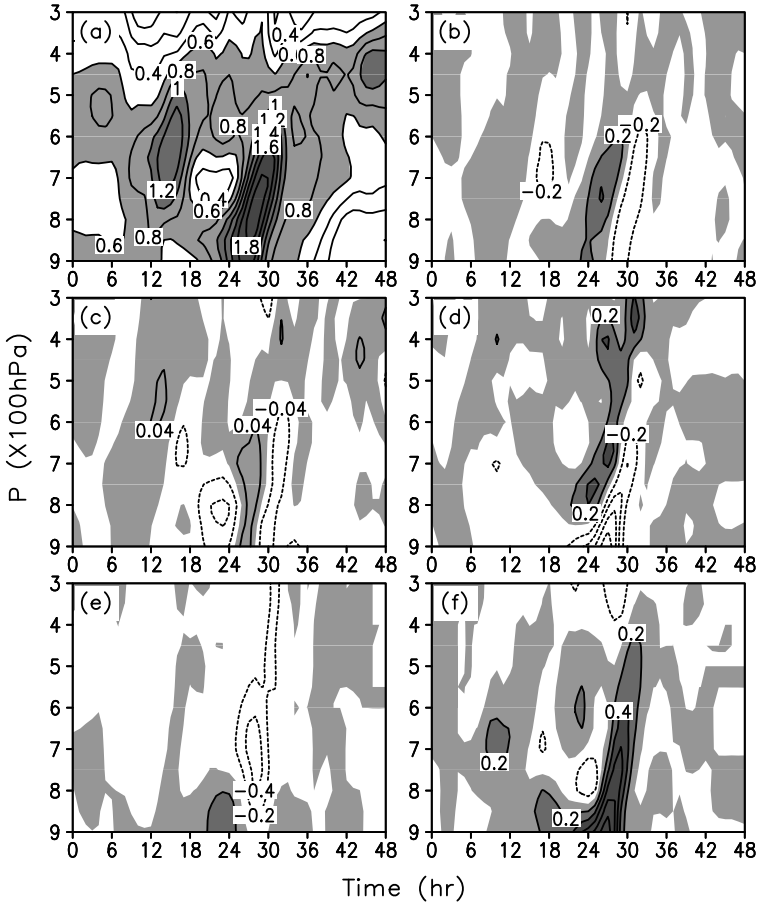

Fig. 9. The time-height sections of PV (units: PUV) and PV budget terms (units: PUV h^{-1}) averaged over an area of $1^\circ \times 1^\circ$ centered at the 850-hPa vorticity maximum (31.2°N, 114°E) of the vortex at τ27: (a) PV, (b) PV tendency, (c) the horizontal flux term, (d) the vertical flux term, (e) the horizontal latent heating effect term, (f) the vertical latent heating effect term. (Shadow: value >0)

9c–f with Fig. 9b, one can see that the vertical distribution of latent heating is the largest individual effect contributing to the total PV tendency. The initial increase of PV at low levels occurs near the low-level moisture front where the significant gradients in the horizontal distribution of latent heat release contributes to the positive PV tendency (Fig. 9e). A comparable contribution arises from the vertical distribution of the latent heating term (Fig. 9e). As the system begins to intensify rapidly around τ22, the upward vertical motion also becomes more intense. In response the vertical flux of PV increases and becomes a significant positive contribution to the PV tendency at mid levels (Fig. 9d). Almost immediately thereafter the low-level PV begins increasing rapidly. The dominant contributing mechanism here, as well as the one augmenting the vertical flux at mid levels, is the vertical distribution of latent heating (Fig. 9f). Thus, the rapid development of the vortex seemingly reflects a positive feedback between the developing vortex and latent heat release.

Further interpretation of the PV budget equation is presented here to fully explore the effect of positive feedback on the eastward movement of vortex. Since the vertical component of the latent heat effect is the primary contributor to the PV increases at low levels, Eq. (2) and Eq. (3) can be simplified to:

$$\frac{\partial q}{\partial t} \propto -(f+\zeta_p)\frac{\partial \dot{\theta}}{\partial p}\,. \tag{5}$$

In the early stage of development, the air between 700 hPa and 800 hPa is near saturation east of vortex center, with weak ascent. Thus, water vapor begins to condense and release latent heat. Below the level of the maximum heating rate ($-\partial\dot{\theta}/\partial p > 0$), the positive PV ($f + \zeta_p > 0$) and convergent circulation combine to cause a slow increase in q ($\partial q/\partial t > 0$). In turn, this intensifies the moisture convergence near the sur-

face and low-level upward motion. As a result the water vapor transport from the surface to low- and middle-layers and rate of latent heat increase, which then generate a further increase of PV. Note too that the increasingly stronger southwesterly winds to the south of vortex provide a plentiful supply of low-level moisture available for transport to higher levels by the enhanced vertical motion to the east of vortex. This consequent extension to higher levels of the latent heat release increases the gradient in the vertical distribution of heating rate ($|\partial\dot{\theta}/\partial p|$) at middle and low layers. As a result, the positive contribution to PV generation by the vertical latent heating term at low levels is enhanced further and its influence extended vertically to middle layers.

From this discussion it should be clear that the release of latent heat acting upon a center of pre-existing positive vorticity can generate a feedback loop resulting in a non-linear increase of low-level PV manifested in rapid intensification of the vorticity. As mentioned, a sufficient and renewable local moisture supply at low levels is crucial for sustaining this positive feedback process. In particular, the maximum in moisture transport from the southwest focus upon the region east of vortex center where the maximum convergence and ascent at low levels are located. Thus the most pronounced latent heat feedback occurs in this sector of the vortex circulation and, therefore, is where the steadily increasing PV is largest. This contributes to the eastward motion of the vortex, as well as to vortex intensification as long as the moisture supply is sufficient.

The process eventually becomes self limiting as the intensifying vortex circulation begins to draw dry sinking air from the northwest over the vortex center. This suppresses the low-level ascent and eventually cuts off the moisture supply. The feedback process diminishes and ceases to be a factor in PV tendencies to the west of the vortex center initially and then over the region to the east.

3.4 *Sensitivity experiment result analysis*

In this section, the sensitivity experiment results are discussed. In EXP1, the model was run without latent heat release over the entire model domain. Consequently, no rain occurs in China, and the center of low pressure, as a reflection of the low-level vortex erodes to a trough (not shown). Clearly, then, latent heating is critical to the intensification of the vortex.

Figure 10 shows the observed and the simulated 24-hour accumulated rainfall by EXP0, EXP2, and EXP3. In EXP2, the low-level water vapor in the southwest area is not allowed to exceed 70%. When the vortex is stalled in Southwest China, the western rainfall is much less than that in EXP0 (Figs. 10b and 10c). But, the eastern rainfall is nearly the same, which supports the argument that the precipitation in this area is not relative to vortex development. Once the vortex moves out of this region, the northeast-southwest oriented rain belt in EXP0 (Fig. 10f) is not reproduced in EXP2 (Fig. 10g). This supports the idea that the water vapor in the southwest area significantly impacts development of vortex and rainfall downstream.

In EXP3, the latent heating is neglected only in the southwest area. In comparison with EXP0, the early western rainfall is significantly less (Fig. 10d), and the southwest part of the rain belt is also much less during the last 24 hours (Fig. 10h). These results are similar with those of EXP2, which indicates that the water vapor has contributions to the feedback effects on the intensification of the vortex by latent heat release in the southwest area. However, in contrast to EPX2, there is rainfall in EXP3 over the Yangtze River and Huaihe River valleys after the vortex moves downstream (Fig. 10h). This indicates that the moisture transport from the southwest area also has a prominent role in sustaining development of the vortex.

By examining the evolution of differences between EXP2 and EXP0 (not shown) in the vertical structure around the vortex center, it was found that the water vapor around the vortex is significantly reduced when the relative humidity is constrained in the southwest area. This considerably reduces the upward-transport of moisture to higher levels. As a result, development of the vortex system is constrained from the very beginning, which subsequently has a direct influence on the "moisture-carrying" capability of the vortex from low layers. As the vortex moves eastward, the weak cyclonically convergent circulation provides a reduced supply of moisture at low layers. The weak ascent blocks the upward moisture transport and lessens the latent heating at middle and high levels. It will restrict the feedback of latent heating, and the vortex intensity is further impaired during its eastward movement.

Differences between EXP2 and EXP0 suggest that a sufficient low-level moisture supply is crucial to the degree of feedback between the latent heating and the vortex development, which in turn direct influences the extent of subsequent vortex strengthening and moisture transportation.

In EXP3, with condensational heating not included, region-SW only, vortex intensification is also suppressed in Southwest China. However, given the high moisture content in the southwest area, there is more water vapor transport downstream in EPX3 than EXP2. This provides an opportunity for initiating the feedback process as the vortex migrates downstream

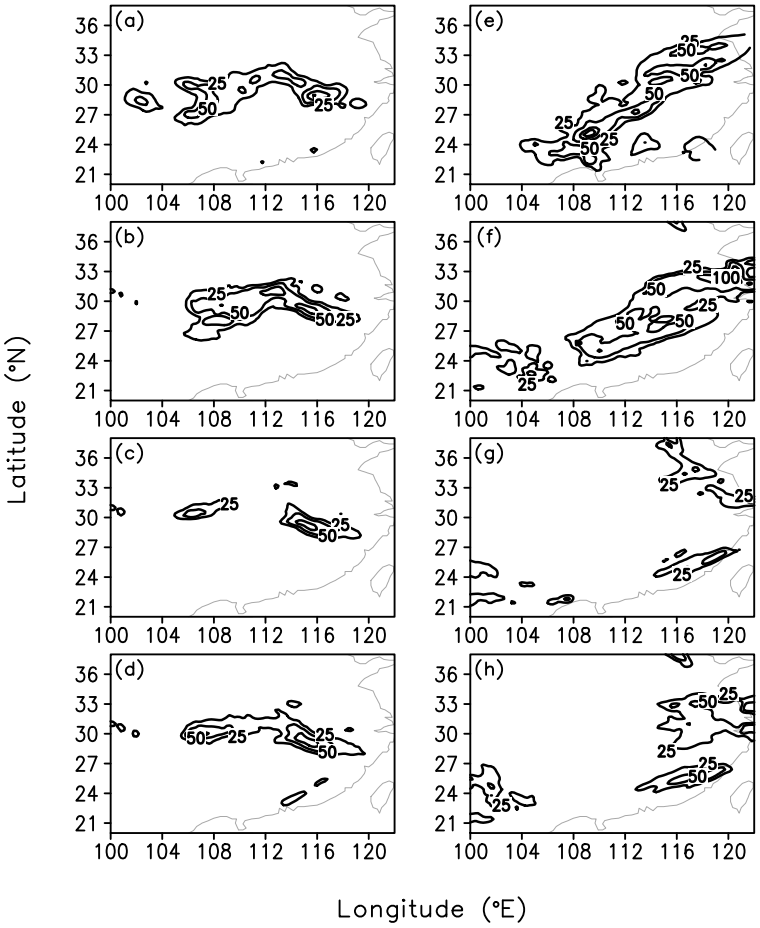

Fig. 10. The 24-hour accumulated rainfall (units: mm) of (a) observation, (b) EXP0, (c) EXP2 and (d) EXP3 from 0000 UTC 25 (τ00) to 0000 UTC 26 (τ24) June 2003. (e), (f), (g), and (h) are the same as (a), (b), (c) and (d) but from 0000 UTC 26 (τ25) to 0000 UTC 27 (τ48) June 2003.

and rainfall increases and the vortex redevelops. At this time, the effects of latent heating in the southwest area primarily influence development of the contiguous cold front southwest of vortex, such that the largest distinction in rainfall between EXP3 and EXP0 is along the cold front, rather than around the vortex center downstream.

From these two sensitivity experiments one can see that, in addition to the supply of low-level moisture, the more intense the vortex before moving eastward the more active the latent heating feedback affecting vortex development as it migrates eastward.

4. Conclusions and remarks

In this paper, we have analyzed an eastward moving vortex during the Meiyu period of 2003 in order to discuss the effect of water vapor from Southwest China on the vortex development and the rainfall downstream. Both the dynamic feedback of the water vapor and the moisture transport from the southwest area are investigated. Water vapor budget analysis by the NCEP data demonstrates that water vapor transported by the southwesterly winds south of the vortex to the downstream area increases the local moisture reserve there. It thereby provides a necessary ingredient for initiating and maintaining a positive feedback of latent heat release upstream aiding in the development of an eastward moving vortex. As shown by model sensitivity experiments, both the low-level moisture supply and the initial vortex strength have impacts on the intensity of this feedback, which in turn directly influences the development and the "moisture-carrying" capability of the vortex during its eastward movement.

In this case study the water vapor in Southwest China is the major moisture source for the downstream rains. The original source of this moisture may be the Bay of Bengal through transport by the westerly

airflow around the southern periphery of the Tibetan Plateau to the Yunnan-Guizhou Plateau. It is then available to the dynamic feedback on an eastward moving vortex. Clearly, then, water vapor in Southwest China is a very important factor in the synoptic scale for the development of these systems and, therefore, a very important factor which requires attention in the prediction of such events. The moisture transport from the South China Sea and the east ocean become available about one day later and are less significant.

A PV budget diagnosis based on the NCEP analysis and model simulations, are used to assess the latent heating effect on the development and eastward movement of vortex. It is demonstrated that the latent heating associated with the 500-hPa stationary trough over the eastern Sichuan Basin initially increases the low-level PV and enhances the cyclonic circulation at low layers. These consequent changes in the circulation results in intensified northeasterly winds and terrain lifting along the sloping mountains in the western basin. With abundant moisture available, convection is triggered. The enhanced cyclonic circulation shifts the convection southeastward along the mountains in the southern basin to the northeastern Yunnan-Guizhou Plateau, where it deposits plenty of water vapor at low levels. A positive feedback between the latent heat release and vortex development commences, which results in rapid intensification of the vortex system as it evolves to its mature stage after 1800 UTC 25 June. Until 0000 UTC 26 June, the transport of moisture northeastward by the strong southwesterly winds to the south of the mature vortex results in gradual extension of the center of high moisture to the east of vortex. This area coincides with the strongest convergence and ascent region around the vortex center such that the maximum latent heat feedback occurs there and contributes to the vortex moving eastward. Hence, the latent heating effect plays a role in both the development and eastward motion of the vortex.

In summary:

(1) The sufficient supply of low-level moisture is essential to initiate a positive feedback process between the latent heat release and the growth of the positive vorticity system at low levels. Such feedback is crucial to the rapid vortex development.

(2) The dominant configuration between the vortex circulation and the moisture supply facilitates the consistent formation of the maximum feedback effect center to the east of vortex center, which makes the vortex propagate eastward.

The intensification of the SW-vortex studied here is very similar to the development of a SW-vortex previously discussed by Wang (1987), where a weak disturbance moved off the Plateau to the conditionally moist unstable air at low layers. It is also similar to the study by Wang (1993) of the development of a mesoscale vortex caused by the diabatic heating associated with MCS (Mesoscale Convective System). The latent heat release plays a direct role in the development and eastward motion of the vortex through the effects of vertical latent heating rate gradient at low levels. This feedback effect is somewhat different from the "self-development" (Sutcliffe and Forsdyke, 1950) of the extratropical cyclone discussed by Uccellini (1990) and Martin et al. (1993) that says the latent heat release may indirectly intensify the "self-development" through the increased cyclonic vorticity advection (CVA) arising from heating the middle troposphere downstream of the upper trough axis.

We acknowledge that additional cases of eastward moving systems should be studied to generalize the description here of favorable circulation and moisture conditions and dynamical mechanisms. This should contribute to increased understanding of eastward movement systems and provide a reference for the assessment and improvement of numerical model predictions.

Acknowledgements. We are grateful to Prof. Zhou Xiaoping from IAP/CAS for his patient help to the first author. This paper was supported by CAS International Partnership Creative Group "The Climate System Model Development and Application Studies". This work was also jointly supported by the Major State Basic Research Development Program of China (973 Program) under Grant No. 2004CB418304.

REFERENCES

Barnes, S. L., 1973: Mesoscale objective map analysis using weighted time series observation. NOAA Tech. Memo ERL NSSL-62, National Severe Storm Laboratory, Norman, OK 73069, 60pp.

Betts, A. K., 1986: A new convective adjustment scheme, Part I: Observational and theoretical basis. *Quart. J. Roy. Meteor. Soc.*, **112**, 677–691.

Chen, Z. M., L. M. Xu, W. B. Min, and Q. Miao, 2003: Relationship between abnormal activities of southwest vortex and heavy rain upper reach of Yangtze River during summer of 1998. *Plateau Meteorology*, **22**(2), 162–167. (in Chinese)

Ding, Y. H., 1989: *Diagnostic Analysis Motheds in Weather Dynamics*. Science Press, Beijing, 293pp. (in Chinese)

Emanuel, K. A., M. Fantini, and A. J. Thorpe, 1987: Baroclinic instability in an environment of small stability to slantwise moist convection Part I: Towdimensional models. *J. Atmos. Sci.*, **44**, 1559–1587.

Gao, K., and Y. M. Xu, 2001: A simulation study of struc-

ture of mesovortexes along Meiyu front during 22–30 June 1999. *Chinese J. Atmos. Sci.*, **25**(6), 740–756. (in Chinese)

Ghan, S. J., J. W. Lingaas, M. E. Schlesinger, R. L. Mobley, and W. L. Gates, 1982: A documentation of the OSU Tow-level Atmospheric General Circulation Model. Report No. 35, Climate Research Institute, Oregon State University, 395pp.

Holtslag, A. A. M., and B. A. Boville, 1993: Local versus nonlocal boundary-layer diffusion in a global climate model. *J. Climate*, **6**, 825–1842.

Hu, B. W., and E. F. Pan, 1996: Tow kinds of cyclonic disturbances and their accompanied heavy rain in the Yangtze River valley during the Meiyu period. *Journal of Applied Meteorological Science*, **7**(2), 138–144. (in Chinese)

Huang, R. H., Z. Z. Zhang, G. Huang, and B. H. Ren, 1998: Characteristics of the water vapor transport in East Asian monsoon region and its difference from that in South Asian monsoon region in summer. *Chinese J. Atmos. Sci.*, **22**(4), 460–469. (in Chinese)

Martin, J. E., J. D. Locatelli, and P. V. Hobbs, 1993: Organization and structure of clouds and precipitation on the mid-Atlantic coast of the United States. Part VI: The synoptic evolution of a deep tropospheric frontal circulation and attendant cyclogenesis. *Mon. Wea. Rew.*, **129**, 748–765.

Mesinger, F., 1984: A blocking technique for representation of mountains in atmospheric models. *Rivista di Meteorologia Aeronautica*, **44**, 195–202.

Raymond, D. J., 1992: Nonlinear balance and potential-vorticity thinking at large Rossby number. *Quart. J. Roy. Meteor. Soc.*, **118**, 987–1015.

Sun, J. H., J. Wei, X. L. Zhang, H. Chen, S. X. Zhao, and S. Y. Tao, 2004: The abnormal weather in the summer 2003 and its real-time prediction. *Climatic and Environmental Research*, **9**(1), 203–217. (in Chinese)

Sutcliffe, R. C., and A. G. Forsdyke, 1950: The theory and use of upper air thickness pattern in forecasting. *Quart. J. Roy. Meteor. Soc.*, **76**, 189–217.

Tao, S. Y., and Y. H. Ding, 1981: Observational evidence of the influence of Qinghai Xizang (Tibet) Plateau on the occurrence of heavy rain and severe convective storms in China. *Bull. Amer. Meteor. Soc.*, **62**, 23–30.

Tao, S. Y., and L. X. Chen, 1987: A review of recent research on the East Asian summer monsoon in China. *Review of Monsoon Meteorology*, Oxford Univ. Press, 60–92.

Uccellini, L. W., 1990: Processes contribution to the rapid development of extratropical cyclones. *Extratropical Cyclones*: *The Erik Palmén Memorial Volume*, C. W. Newton and E. O. Holopainen, Eds., Amer. Meteor. Soc., 81-105.

Wang, B., 1987: Study of a heavy rain vortex formed over the eastern flank of the Tibetan Plateau. *Mon. Wea. Rev.*, **115**, 1370–1393.

Wang, W., 1993: A diabatically driven mesoscale vortex in the lee of the Tibetan Plateau. *Mon. Wea. Rev.*, **121**, 2542–2561.

Xu, Y. P., D. Q. Xia, and Y. Y. Qian, 1998: The water-bearing numerical model and its operational forecasting experiments Part II: the operational forecasting experiments. *Adv. Atmos. Sci.*, **15**(3), 321–336.

Yu, R. C., 1994: A tow-step shape-preserving advection scheme. *Adv. Atmos. Sci.*, **11**(4), 479 -490.

Yu, R. C., 1995: Application of a shape-preserving advection scheme to the moisture equation in an E-grid regional forecast model. *Adv. Atmos. Sci.*, **12**(1), 13–19.

Yu, R. C., and Y. P. Xu, 2004: AREM and its simulation on the daily rainfall in summer in 2003. *Acta Meteorologica Sinica*, **62**(6), 715–724. (in Chinese)

Zeng, Q. C., 1963: Characteristic parameters and dynamic equation of the atmospheric movement. *Acta Meterologica Sinica*, **33**, 472–483. (in Chinese)

Zeng, X. B., M. Zhao, and R. E. Dickinson, 1998: Intercomparison of bulk aerodynamic for the computation of sea surface fluxes using TOGA COARE and TAO Data. *J. Climate*, **11**, 2628–2644.

Zhang, Q. Y., S. Y. Tao, and S. L. Zhang, 2003: The persistent heavy rainfall over the Yangtze River valley and its associations with the circulations over East Asian during summer. *Chinese J. Atmos. Sci.*, **27**(6), 1018–1030. (in Chinese)

Zhang, Q. Y., H. J. Wang, Z. H. Lin, J. H. Sun, X. L. Zhang, and J. Wei, 2004: *Studies on the Causes of Anomalous Weather and Climate over China in 2003*. China Meteorological Press, Beijing, 170pp. (in Chinese)

Zhou, T. J., and R. C. Yu, 2005: Atmospheric water vapor transport associated with typical anomalous summer rainfall patterns in China. *J. Geophys. Res.*, **110**, D08104, doi:10.1029/2004JD005413.

Zhou, Y. S., S. T. Gao, and G. Deng, 2005: A diagnostic study of water vapor transport and budget during heavy precipitation over Changjiang River and Huaihe River basins in 2003. *Chinese J. Atmos. Sci.*, **29**(2), 195–204. (in Chinese)